# WASTE2ROAD

Biofuels from WASTE TO ROAD transport

LC-SC3-RES-21-2018 (818120)

# Deliverable Report

| | | | |
|---|---|---|---|
| **Deliverable ID** | D3.12 | | |
| **Deliverable name** | Report on the contaminants level, characteristics, and valorisation after primary processing | | |
| **Lead beneficiary** | VTT - Christian Lindfors, Elmeri Pienihäkkinen, Taina Ohra-aho, Anja Oasmaa | | |
| **Contributors** | BTG, CNRS, CEA | | |
| **Due date Annex 3** | January 31, 2022 (M40) | | |
| **Date of final version** | 14.03.2022 | | |
| **Dissemination level** | Public | | |
| **Document approval** | Duncan Akporiaye | 14.03.2022 | |

This project has received funding from the European Union's Horizon 2020 research and innovation programme under grant agreement No 818120.

# Description of the deliverable content and purpose

**Task 3.6. Contaminants (M6-M42) (VTT, BTG, CEA, CNRS).**
A crucial aspect is to reduce the inorganic contaminant level (other than the organic oxygen) in bio-liquids, especially if they are prepared from waste materials. **The objective of the task 3.6 is to investigate the effect of different contaminants present in biomass waste (such as in the contaminated wood or in municipal wastes) on the quantity and quality of the primary bio-oils and / or downstream fuels.**

Main constraints associated with the use of pyrolysis oils, or FPBO, in co-refining are related to the bio-oil contaminants, especially alkali metals and sulphur, as these are considered harmful for cracking catalyst. It is obvious that accurate, reliable, and reproducible analytical methods are needed to formulate the basis of specifications/standard for refinery feed. Several analytical test methods have already been developed and validated (1) but more work is needed to create accurate analytical methods for low amounts of S, Cl, N, alkaline and earth alkaline metals (AEAM), and other metals. Reasonable limits for the contaminants could be total alkali metal content < 50 ppm, sulphur content < 10 ppm, chlorine < 50 ppm, and nitrogen < 0.1 %. Here, a summary of analytical methods is described. More detailed description is found in D3.7.

In fast pyrolysis most of the inorganic material are retained in the char and released in the form of ash in the flue gas recovery section. In upstream hydrotreating processes, water with organics will be produced. Where possible the waste streams should be valorised, and this requires detailed analyses. In Waste2Road, ash metal analyses will be carried out both for feeds and for bio-liquids to determine the efficiency of ash and metal removal (primarily by ICP/VTT), while ex-situ techniques to remove contaminants possibly detrimental for further upgrading in WP3 will be investigated by BTG (food residue, ex-situ), VTT and CNRS (contaminated wood and municipal wastes, in-situ). Feedback with hydrotreating and co-FCC processing, both in WP4, will be established, to assess, for example, the effect on the respective catalyst performance. Valorisation of contaminants concentrated in the ash from pyrolysis will be investigated by VTT, and the removal of organics in any aqueous phase by BTG.

In HTL, water is produced that is rich in organics and inorganics. The valorisation of the organics to produce hydrogen will be examined by supercritical water gasification (Task 4.3). The inorganics will be concentrated in a brine. The process also produces a concentrated carbon dioxide stream that may be available for sequestration or valorisation. The task will analyse all the different process streams to propose a valorisation of each of the stream.

# Table of Contents

# 1 Materials and methods

## 1.1 Materials

In the project various biomasses and waste sources were chosen for fast pyrolysis or hydrothermal liquefaction (HTL):

- Industrial residual (contaminated) wood from Twence and L&T for pyrolysis
- Roadside grass from Twence for pyrolysis
- Food residue pretreatment reject from bioreactor for pyrolysis from REG
- Food residue from canteens for HTL
- FFOM: Organic fraction of municipal waste from Suez for pyrolysis and HTL
- Digestate from REG for pyrolysis and HTL
- Sunflower husk from Ukraine for pyrolysis
- Black liquor for HTL

## 1.2 Analytical methods for contaminants

Analytical test methods for FPBO have been developed since 90's, with VTT as a key stakeholder (2,1,3,4). The test methods have been validated by several IEA round robins (5,6,7,8). Based on this work applicable test methods can be recommended for fast pyrolysis bio-oils with certain additions. These analytical test methods form the basis of present FPBO standards (ASTM D7544:2017, EN EN16900:2017). However, for new standards some different analyses as well as those determining accurately lower amounts are now needed.

Limited validation work has been done for S, Cl, N, and metals in FPBOs and even less with hydrothermal liquefaction biocrudes. One recent round robin study (5) evaluating the analysis of bio-liquids from fast pyrolysis and hydrothermal liquefaction (HTL) was performed by IEA Bioenergy Task 34. The results suggested that the analytical methods used by the various laboratories should be compared, the most suitable one developed further to provide accurate characterisation of these elements, and a new round robin for the validation of the developed methods to be carried out. This is crucial to proceed with preparation of new standards.

**CHN**. An elemental analysis of carbon, hydrogen and nitrogen is carried out according to ASTM D 5291. At least triplicates and representative standards are recommended for characterisation of bio-liquids (1). Oxygen (dry basis) is calculated by difference. The detection limit of the method can be an obstacle, for example, in determining low amounts of nitrogen.

**Sulphur.** ASTM D5453 is presently recommended to measure sulphur content of FPBOs. However, this method is still under development and validation.

**Chlorine.** There is not yet any recommended method for chlorine determination. At VTT Cl is determined by coulorimetric titration using an Xplorer TX equipment. The equipment fulfil requirements of method ASTM D4929 Organic Chloride Content in Crude Oil. However, the methods need to be still developed and validated for bio-oils. Downside of the method is that it does not differentiate chlorine from other halides present in the sample.

**Ash content.** At VTT ash content is measured according to standard EN/ISO 6245 (EN7). In case of FPBOs, a small modification to the ash content method is recommended: sample crucibles of 150 ml (width 80 mm, height 55 mm) should be used to avoid splashing of the sample. The addition of isopropanol or ash-free filter paper for absorbing the water can also prevent splashing (1). A rapid ash analysis has been developed at VTT where first MCR is determined after that the sample is combusted to get ash (D3.7). Same results than with the standard has been obtained. At BTG ASTM D482 method is used.

**Alkali metals.** Alkali metals are typically analysed by ICP-OES (Optical Emission Spectroscopy) according to EN 16476. In the standard the sample is dissolved in kerosene. With FPBOs the solvent is recommended to be replaced by methanol because of the solubility of FPBO. This might also require some material changes in ICP-OES. Another option is to dissolve the FPBO in a mineral acid before analyses.

There is need to robust and quick analysis standards, that are useful and applicable for refinery applications as well. These type of methods would be needed especially to MCRT (ASTM D 189 or ASTM 4530), carbonyl content (ASTM E3146) and XRF techniques. Discussion on XRF is presented in Appendix 1.

# 2 Primary and secondary processes

## 2.1 Fast pyrolysis and hot-vapour filtration at VTT

FPBO from contaminated wood was produced at VTT using both bench and pilot units. Before the experiments, the feedstock was grinded and sieved to a particle size of 0.25-3 mm and dried to a moisture content close to 8 wt%. Before the bench-scale experiments, feedstock was grinded further and sieved to a particle size of 0.5-1 mm. In the bench-scale (1 kg/h), a bubbling fluidized bed reactor was used (Figure 2.1). The fluidization agent was nitrogen, the pyrolysis temperature 480-520 °C, and the gas phase residence time 1 s. The char left after pyrolysis was separated from the gases with two cyclones. After the cyclones, the hot vapours and gases were quenched rapidly in the liquid recovery system by three coolers and one electrostatic precipitator. The composition of the non-condensable gases was analysed by gas chromatography.

A set of pyrolysis experiments were carried out in bench-scale using the hot vapour filtration to investigate the metal removal before liquid condensation. For these experiments a hot vapour filter was added in the line between the cyclones and liquid recovery system. Operational concept of the new hot vapour filter developed at VTT is based on combining a barrier filter with a moving med filter. In the experiments, the filtration temperature, filter face velocity and filtration residence time were varied to optimize the organic liquid yield. The performance of hot-vapour filtration unit is described in D3.11.

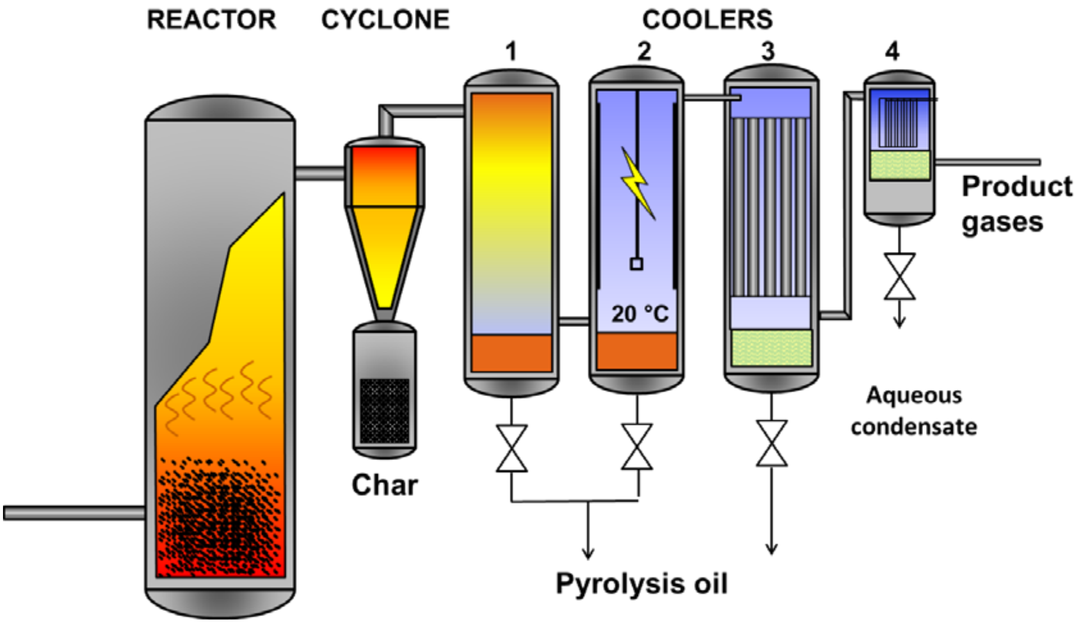

*Figure 2.1. Schematic flow diagram of the bench-scale fast pyrolysis unit at VTT.*

In VTT's pilot (20 kg/h) unit the grinded and sieved (0.25-3 mm) raw material was fed into the reactor with screw feeder (2.2). The reactor is a circulated fluidized bed heated with the hot sand from the combustor. The target pyrolysis temperature was 480-520 °C, and the residence time for pyrolysis vapours 0.9-1.7 s. The main part of the char particles as well as heat transfer sand is removed from the hot product gases and vapours by two cyclones before entering the liquid recovery system containing two scrubbers and one cooler. In the liquid scrubbers the vapour is condensed using the product liquid as a cooling agent. The temperature of the scrubbers was kept at 40 and 55 °C to obtain one reference bio-oil and one bio-oil with lower moisture content. A part of the non-condensable gases is used for fluidization and the rest is burned in the combustor. Most of the ash from the feedstock ends with the char in the combustor. The combustor is operated as a bubbling fluidized bed and the temperature is controlled to 650-700 °C by feeding grinded pellets into it. After the combustor one cyclone and a hot gas filter is used to remove the fine dust and fly ash from the flue gases. Before the hot gas filter, flue gas is cooled to <250 °C using tube heat exchanger and water quench.

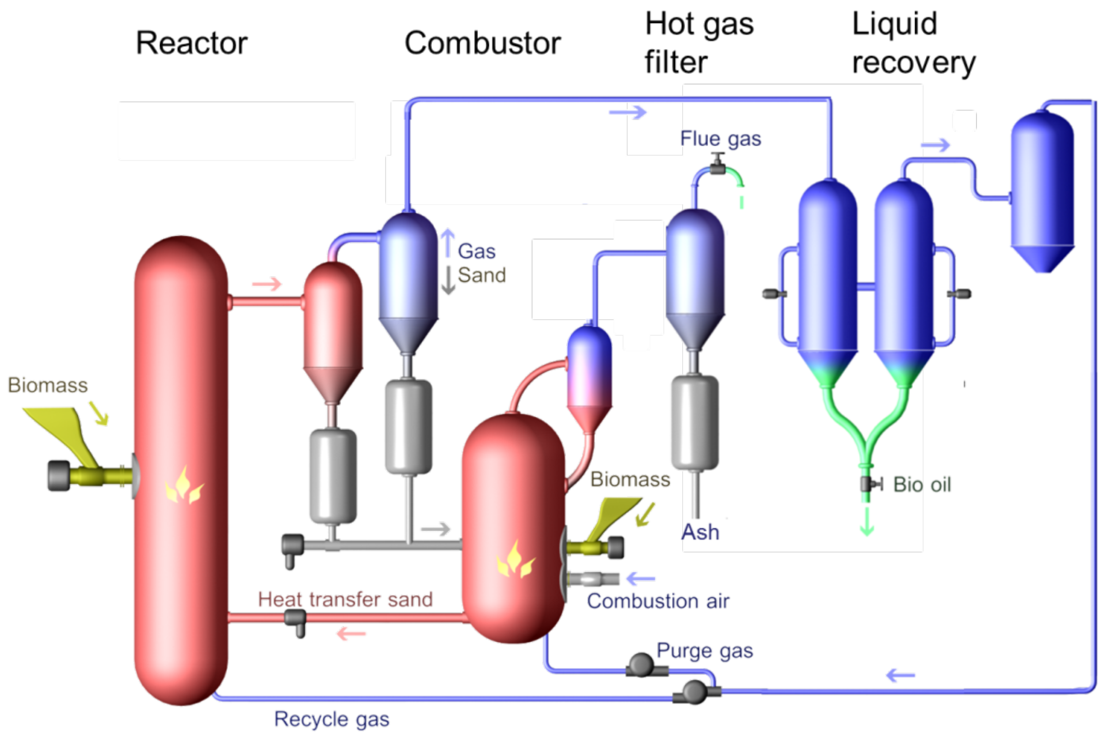

*Figure 2.2. Schematic representation of VTT's pilot (20 kg/h).*

## 2.2 Fast pyrolysis and secondary processes at BTG

### 2.2.1 Fast pyrolysis

The pyrolysis plants at BTG are designed according to a rotating cone principle and appear a valid representation of the commercial scale processes. The rotating cone reactor efficiently mixes biomass and hot sand as a circulating heat carrier material. After rapid heating applying short gas-phase residence times, biomass is converted into pyrolysis oil vapors, incondensable gases and char. These products are then subsequently separated into two streams. The char is entrained by the sand, and fed to the char combustor. Air is used the char to be combusted and the sand to be re-heated and recycled back to the reactor. The produced vapors and gasses pass several cyclones and fed into the condenser where they are quickly quenched. The schematic illustration of the process is shown on Figure 2.3.

The larger pilot plant has a capacity of ~150 kg/h and was used to obtain the larger batch of bio-liquid while a smaller bench-scale unit with a throughput of ca 5 kg /h was used to perform additional experiments.

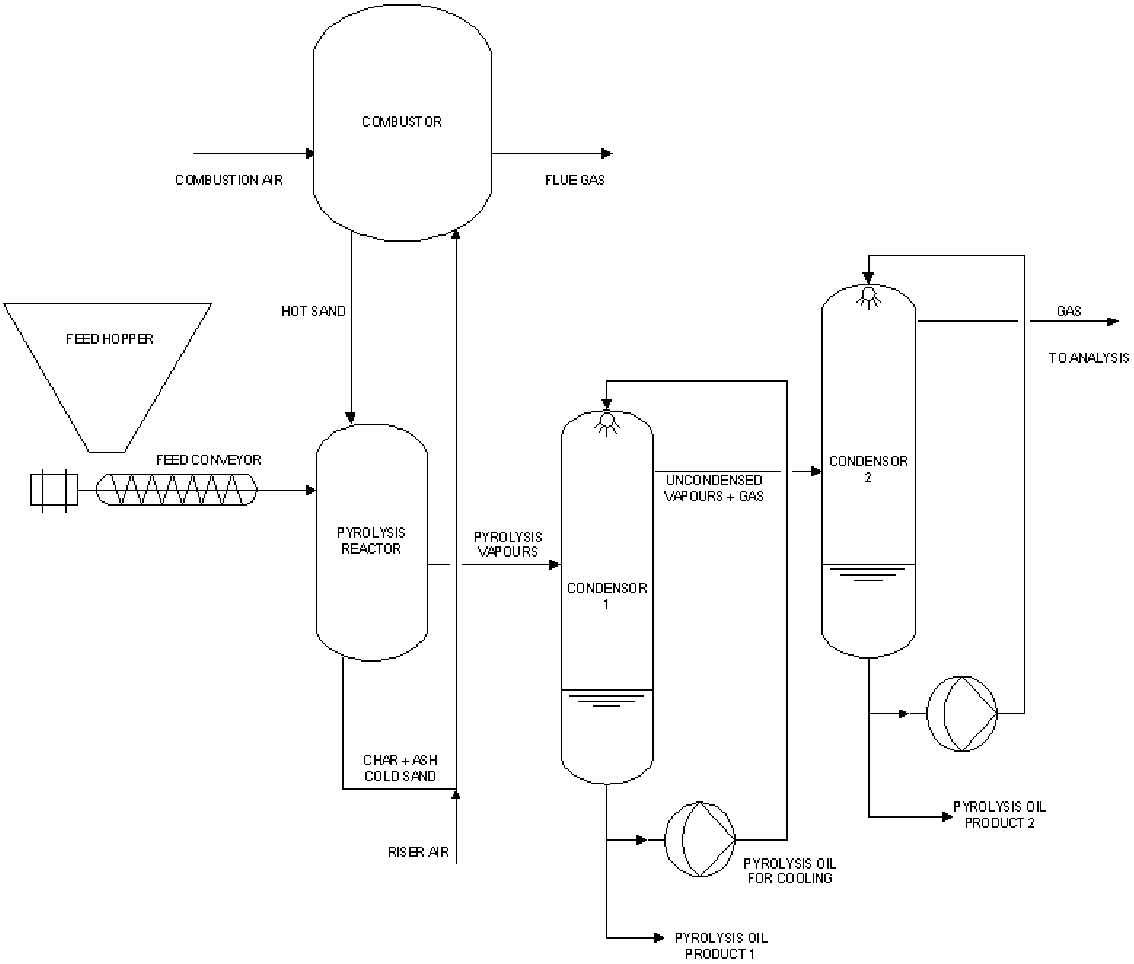

***Figure 2.3*** *Schematic illustration of fast pyrolysis units at BTG.*

Characterization of the FPBO is carried in BTG's lab using (some modified) standard methods for the most critical elements of the FPBO only.

- Elemental composition using a Eurovector 3000 Elemental Analyzer. Heating values were calculated from the elemental composition using the Milne formula.
- Moisture content by Karl Fischer Titration using Metrohm 719 S Titrino and Sigma-Aldrich KF reagents.
- MCRT according to ASTM 4530 using an Alcor Micro Carbon Residue Tester.
- Acid number was defined by a modified ASTM D664 and Metrohm 848 Titrino plus.
- Ash content was calculated according to ASTM D482 and incineration in Carbolite AAF 1100 oven
- Solids content using a modified ASTM D3977 and 4 µm Whatman filter papers.
- To determine pH ASTM E70 test with glass electrode was performed.

## 2.3 Lab scale pyrolysis bench at CNRS

The lab-scale pyrolytic setup used at CNRS was developed and built previously in the laboratory, and adapted to the W2R project. The dry biomass is placed in a gas tight hopper where it is swept by a $N_2$ flow (260 mL/min) to prevent water adsorption on the wood chips and to drive the pyrolysis vapours towards the catalytic bed. A solid dispenser feeds the biomass semi-continuously into the reactor by small increments every 10.4 seconds, resulting in a global feeding rate of approximately 20 g/h. The wood chips fall by gravity in a quartz tubular reactor equipped with internal spikes to slow their fall and to increase the residence time of biomass particles in the pyrolysis section (Figure 2.4), which is heated at ≈500 °C by a tubular furnace. At the bottom of the pyrolysis zone, a quartz frit collects the solid chars and ashes. Just below, the catalytic bed is supported by a second quartz frit. At this stage, a second inert flow composed of 240 mL/min $N_2$ and 20 mL/min He (internal standard for gas chromatography) is added to prevent retro-diffusion and to adjust the residence time of vapours.

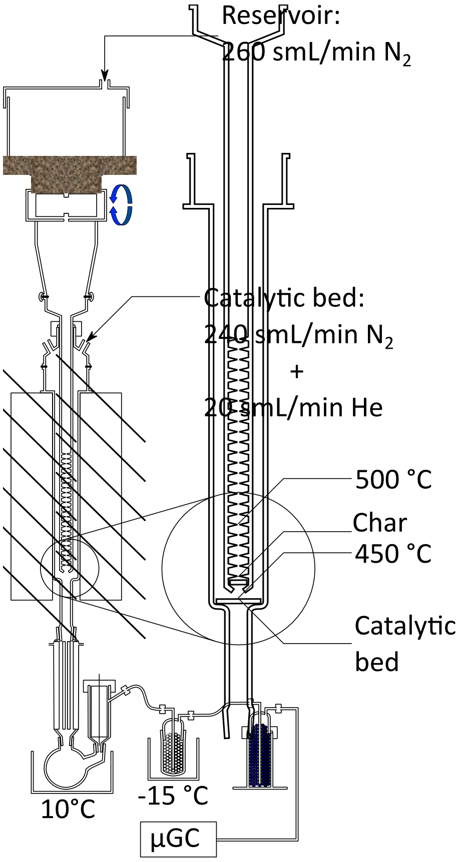

*Figure 2.4 Schematic illustration of Pyrolysis bench scheme*

The gaseous products are analysed online using a micro gas chromatograph (µGC). The condensable products are recovered in a sequence of traps composed by a (1) condenser and (2) round bottom flask at 10 °C, (3) electrostatic precipitator, (4) trap filled with glass beads at -15 °C, and (5) silica gel bead trap at ambient temperature aiming to prevent condensable compounds to be pumped into the µGC injection valves. The solid and liquid products are analysed by different analytical techniques.

## 2.4 HTL at CEA

The biocrudes in the project Waste2Road were produced in a batch reactor in screening experiments and in a continuous unit for larger scale production. Initial screening showed that for most resources of type FW (collected from the company restaurant H1) a temperature of 300°C and above gives the best results.

*Figure 2.5. Batch HTL Reactor (left) and continuous HTL reactor (right)*

Liquefaction in batch autoclaves does not require any special measures. However, in the continuous unit suspensions are prepared in advance stored during several hours especially during the night for longer experiments. To avoid precipitation in the storage and transfer lines xanthane gum was mixed into the powdered resources. The use of 0.1-0.2 % of xanthane in a mixture gives good stable suspensions with a very limited effect on the results.

The reactor, as shown in 2.6, consists of a set of tanks, pumps (P1 and P2) and the reactor itself. In a typical test, the reactor is heated to test conditions before injecting the biomass. The water circulation is established from the "Water 1" tank to be sent to the "Water 2" tank with the reactor heating system in operation. The tubular reactor is horizontal with six heating elements with an installed power of 2 kW. Pumps P1 regulate the flow rate while pumps P2 regulate the pressure. Once the system is stable and at the right temperature, the feed is switched to the "BM" biomass feed tank. After 25 minutes in this mode, the output is switched to the "Product" storage tank. In this tank biocrude is directly separated from the water phase by a metallic sieve so that the aqueous phase is recovered at the bottom of the tank and biocrude remains on the sieve. After each experiment, sieves are weighted to calculate conversion yields. The biocrudes is left at ambient temperature for a first drying before analyses.

During the test, the temperature is monitored by thermocouples, TCx, shown in the diagram below. Monitoring the temperature upstream and downstream of exchanger E is particularly important.

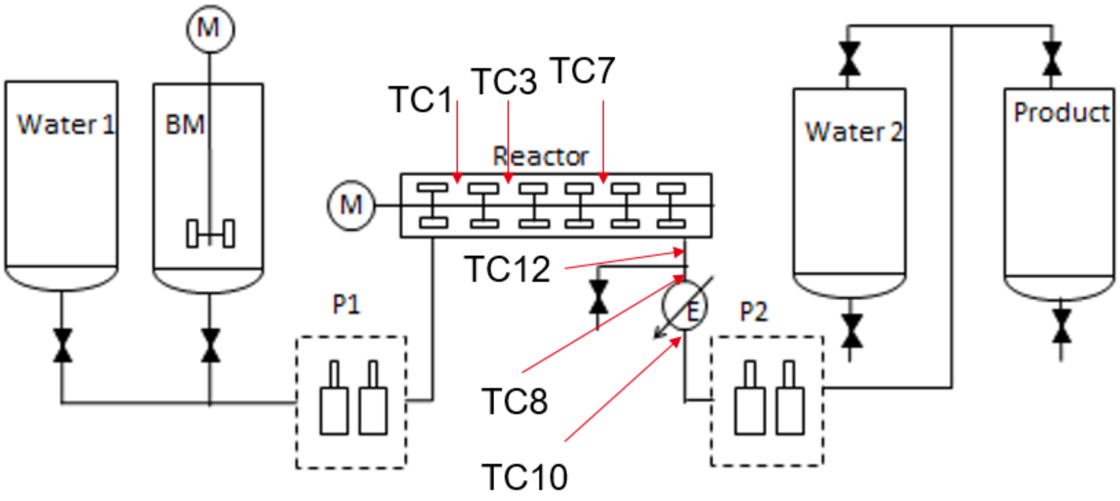

*Figure 2.6. Schematic of the continuous HTL reactor*

The temperature measurements are important to be able to monitor the condition of the installation and the progress of a test. When the biocrude is too viscous, outlet temperatures rise. The oils then become less viscous and a stable equilibrium state is found (most of the times). If the biocrude remains too viscous, the exchanger can plug before finding a steady regime.
Tank "BM" was originally a single day tank with a capacity of 15 L. It is now doubled with 50 L tank that allows longer overnight experiments.

# 3 Results

## 3.1 Composition of primary liquids

Table 3.1 shows the content of contaminants in primary liquids without hot-vapour filtration or ex-situ processes.Contaminants levels were lowest in reference oil and highest in the oil produced from food waste and FROM.

*Table 3.1. Contaminants in primary liquids without hot-vapour filtration or ex-situ processes.*

| Sample | | Reference oil, Empyro, VTT | Reference oil, Empyro BTL | Contaminated wood | Contaminated wood | Reject | Digestate | Roadside grass | FFOM | Sunflower husk |
|---|---|---|---|---|---|---|---|---|---|---|
| Producer | | BTL | BTL | BTG | VTT | BTG | BTG | BTG | BTG | BTG |
| As | mg/kg, d | <0.5 | 0 | 3.4 | 2 | 0.9 | 2.9 | 0.55 | <0.5 | <0.5 |
| Cd | mg/kg, d | 0.08 | <1 | 0.2 | <0.5 | 0.42 | 0.11 | 0.05 | 0.6 | <0.5 |
| Co | mg/kg, d | <0.5 | 0 | <0.5 | <1 | <0.5 | <0.5 | <0.5 | <0.1 | <1 |
| Cr | mg/kg, d | <0.5 | <1 | 9.5 | 2 | 3.3 | 1.1 | 1.2 | 6 | <1 |
| Cu | mg/kg, d | 0.57 | <1 | 40 | <1 | 26 | 16 | 21 | 24 | 9 |
| Hg | µg/kg, d | <0.02 | <0.01 | 0.09 | <100 | 0.02 | 0.14 | <0.02 | <100 | <100 |

| | | | | | | | | | | |
|---|---|---|---|---|---|---|---|---|---|---|
| Mn | mg/kg, d | 3.4 | 6 | 21 | 8 | 5.7 | 9.2 | 1.6 | 4 | 2 |
| Mo | mg/kg, d | <0.5 | <1 | <0.5 | <5 | <0.5 | <0.5 | <0.5 | <5 | <5 |
| Ni | mg/kg, d | <0.5 | <1 | 2.7 | 1 | 2.3 | 0.95 | 1.1 | 3 | <1 |
| Pb | mg/kg, d | <0.5 | <1 | 17 | <10 | 2.7 | 0.93 | 2.2 | <10 | <10 |
| Sb | mg/kg, d | <0.5 | 0 | <0.5 | 2 | 1.6 | <0.5 | <0.5 | 1 | <0.5 |
| Tl | mg/kg, d | <0.5 | 0 | <0.5 | <0.5 | <0.5 | <0.5 | <0.5 | <0.5 | <0.5 |
| V | mg/kg, d | <0.5 | <1 | <0.5 | <1 | <0.5 | <0.5 | <0.5 | <1 | <1 |
| Zn | mg/kg, d | 1.6 | 2 | 30 | 4 | 20 | 23 | 23 | 28 | 4 |
| Ca | mg/kg, d | 35 | 62 | 670 | 233 | 330 | 1100 | 270 | 1950 | 245 |
| Mg | mg/kg, d | <10 | 20 | 120 | 42 | 21 | 47 | 17 | 178 | 94 |
| Na | mg/kg, d | <10 | 14 | 57 | <10 | <10 | 30 | <10 | 188 | <10 |
| K | mg/kg, d | <10 | 36 | 120 | 147 | 16 | 35 | 210 | 203 | 983 |
| P | mg/kg, d | <10 | 5 | 87 | 25 | 81 | 240 | 89 | 165 | 29 |
| S | mg/kg, d | 67 | 0 | 470 | 271 | 5700 | 10200 | 4300 | 2620 | 1570 |
| Fe | mg/kg, d | 2.4 | 7 | 140 | 81 | 87 | 200 | 36 | 232 | 28 |
| Al | mg/kg, d | <10 | 2 | 120 | 72 | 62 | 120 | 40 | 512 | 72 |
| Si | mg/kg, d | 59 | 5 | 220 | 367 | 160 | 220 | 150 | 1590 | 235 |
| Ti | mg/kg, d | <1 | <1 | 48 | 14 | 13 | 5.4 | 1.1 | 41 | <5 |
| Mn | mg/kg, d | 4.2 | 6 | 22 | 0 | 5.9 | 9.9 | 1.6 | | |
| Ba | mg/kg, d | <1 | <1 | 50 | 3 | <1 | 1 | <1 | 7 | <1 |
| Cl | %, d | 0.006 | <0.001 | 0.031 | 0.0305 | 0.022 | 0.015 | 0.023 | 0.053 | 0.016 |

## 3.2 Pyrolysis and impurity removal of industrial residual (contaminated) wood at VTT

Fast pyrolysis experiments were carried out with contaminated wood from Finland (L&T) and from Netherlands (Twence). The materials have been analysed for fuel properties and metal composition (ICP-MS and ICP-AES).

*Table 3.2. Properties of contaminated wood, on dry basis.*

| **Feedstock description** | **Unit** | **Contaminated wood** | **Contaminated wood** |
|---|---|---|---|
| Feedstock origin | | L&T | Twence |
| Moisture | wt% | 8.0 | 8.5 |
| Volatiles | wt% db | 84.7 | 78.4 |

| | | | |
|---|---|---|---|
| Ash 550 °C | wt% db | 0.8 | 1.9 |
| Carbon | wt% db | 50.4 | 48.8 |
| Hydrogen | wt% db | 6.0 | 5.9 |
| Nitrogen | wt% db | 0.4 | 2.6 |
| HHV | MJ/kg db | 20.2 | 19.8 |
| LHV | MJ/kg db | 18.9 | 18.5 |
| Cl | wt% db | 0.02 | 0.08 |
| S | wt% db | 0.017 | 0.055 |

*Table 3.3. Metal contents of contaminated wood, on dry basis.*

| | Metals | Unit | VTT, Finland 1 | BTG, Netherlands |
|---|---|---|---|---|
| AAEM | Na | mg/kg | 350 | 620 |
| | K | mg/kg | 500 | 750 |
| | Mg | mg/kg | 230 | 650 |
| | Ca | mg/kg | 1700 | 2700 |
| Other metals | Cr | mg/kg | 6.4 | 32 |
| | Mn | mg/kg | 80 | 90 |
| | Fe | mg/kg | 210 | 660 |
| | Cu | mg/kg | 6.4 | 42 |
| | Zn | mg/kg | 58 | 85 |
| | Si | mg/kg | 790 | 1700 |
| | Pb | mg/kg | 20 | 56 |
| | P | mg/kg | 55 | 160 |
| | S | mg/kg | 170 | 550 |
| | Cl | mg/kg | 200 | 820 |

Pyrolysis experiments were carried out with the contaminated wood from L&T in both bench and pilot scale at VTT. During the experiments, temperatures and residence times were varied to maximize the liquid yield. The product yields for the bench and pilot scale experiments is presented in Figure 3.1. Mass balances from both bench and pilot scale were very similar.

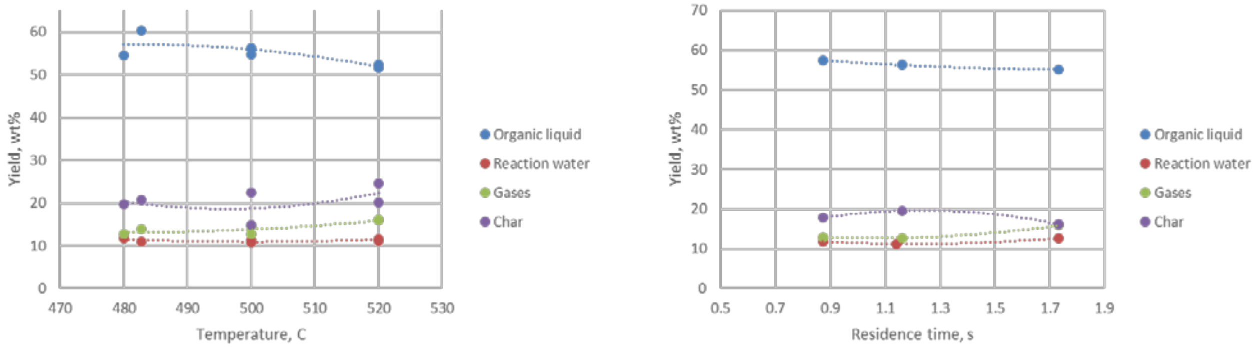

*Figure 3.1. Influence of temperature (left) and residence time (right) on product distribution.*

Metal content from the produced liquid was measured and metal removal calculated Table 3.4. Alkali and alkaline earth metals alongside some other heavy metals were significantly reduced during pyrolysis and only small amounts bypassed the cyclones and ended in the liquid product. Sulphur and chlorine were not significantly reduced in pyrolysis.

*Table 3.4. Metal removal from contaminated wood in fast pyrolysis pilot test.*

| | | Metall content, mg/kg | | | Yield in bio-oil, wt% | | | | |
|---|---|---|---|---|---|---|---|---|---|
| | Metals | Feedstock | Oil product, stages 1-2 | Oil product, stages 3-5 | Stage 1 | Stage 2 | Stage 3 | Stage 4 | Stage 5 |
| AAEM | Na | 350 | 10 | 10 | 2 | 2 | 1 | 2 | 2 |
| | K | 500 | 93 | 22 | 11 | 10 | 2 | 3 | 2 |
| | Mg | 230 | 35 | 17 | 9 | 9 | 4 | 4 | 4 |
| | Ca | 1700 | 150 | 99 | 5 | 5 | 3 | 3 | 3 |
| Other metals | Cr | 6.4 | 1.2 | 0.99 | 11 | 11 | 8 | 9 | 9 |
| | Mn | 80 | 7.5 | 5.3 | 6 | 5 | 3 | 4 | 4 |
| | Fe | 210 | - | - | - | - | - | - | - |
| | Cu | 6.4 | 0.5 | 0.5 | 5 | 4 | 4 | 4 | 4 |
| | Zn | 58 | 1.2 | 2.1 | 1 | 1 | 2 | 2 | 2 |
| | Si | 790 | 180 | 55 | 14 | 13 | 4 | 4 | 4 |
| | Pb | 20 | 0.5 | 1.2 | 2 | 1 | 3 | 3 | 3 |
| | P | 55 | 18 | 10 | 20 | 18 | 10 | 10 | 10 |
| | S | 170 | 190 | 150 | 67 | 63 | 46 | 51 | 49 |
| | Cl | 200 | 370 | 380 | 112 | 104 | 99 | 109 | 105 |
| | **Metal removal, %** | | | | **91** | **92** | **96** | **96** | **96** |

Part of the ash was recovered from the sand heater, where the char is combusted. The composition of the ash is presented in Table 3.5.

*Table 3.5. Metal composition of the ash recovered from the sand heater in the pilot test with contaminated wood.*

| Element | Unit | Stage 1-2 | Stage 3-5 |
|---|---|---|---|
| As | mg/kg | 230 | 230 |
| Cd | mg/kg | 7.8 | 4.5 |
| Co | mg/kg | 21 | 22 |
| Cr | mg/kg | 660 | 900 |
| Cu | mg/kg | 300 | 330 |
| Hg | mg/kg | 1.4 | 2.7 |
| Mn | mg/kg | 7100 | 6500 |
| Mo | mg/kg | 42 | 44 |
| Ni | mg/kg | 450 | 520 |
| Pb | mg/kg | 230 | 810 |

| | | | |
|---|---|---|---|
| Sb | mg/kg | 71 | 76 |
| Ti | mg/kg | 5 | 4.1 |
| V | mg/kg | 70 | 64 |
| Zn | mg/kg | 1200 | 2000 |
| Ca | mg/kg | 129000 | 139000 |
| Mg | mg/kg | 23900 | 24000 |
| Na | mg/kg | 12500 | 19000 |
| K | mg/kg | 19600 | 26000 |
| P | mg/kg | 4600 | 4800 |
| S | mg/kg | 17400 | 17200 |
| Al | mg/kg | 53400 | 55300 |
| Si | mg/kg | 145000 | 155000 |
| Ti | mg/kg | 8700 | 11800 |
| Mn | mg/kg | 6500 | 5900 |
| Ba | mg/kg | 2700 | 3700 |

Metal removal was still improved in bench scale by adding a hot vapour filter between the cyclones and liquid recovery system. Table 3.6 lists the metals content in filtered and unfiltered bio-oil. Only small improvement in metal removal could be seen in the bench scale. Potassium and magnesium quantities were both 10 mg/kg for unfiltered and filtered bio-oils, which was the detection limit for these metals. Small reduction in sodium and calcium could be seen after the filtration.

*Table 1.6. Metal analysis of unfiltered and filtered bio-oil.*

| | | Metall content, mg/kg | | | Yield in bio-oil, wt% | |
|---|---|---|---|---|---|---|
| | Metals | Feedstock | Unfiltered oil | Filtered bio-oil | Unfiltered oil | Filtered bio-oil |
| AAEM | Na | 350 | 84 | 70 | 13 | 10 |
| | K | 500 | 10 | 10 | 1 | 1 |
| | Mg | 230 | 10 | 10 | 2 | 2 |
| | Ca | 1700 | 28 | 10 | 1 | 0 |
| Other metals | Cr | 6.4 | 0.5 | 0.66 | 4 | 5 |
| | Mn | 80 | 1 | 1 | 1 | 1 |
| | Fe | 210 | 18 | 2.4 | 5 | 1 |
| | Cu | 6.4 | 0.5 | 0.5 | 4 | 4 |
| | Zn | 58 | 1.8 | 0.98 | 2 | 1 |
| | Si | 790 | 51 | 14 | 4 | 1 |
| | Pb | 20 | 0.5 | 0.5 | 1 | 1 |
| | P | 55 | 10 | 10 | 10 | 9 |
| | S | 170 | 180 | 110 | 58 | 31 |
| | Cl | 200 | 260 | 190 | 71 | 46 |
| | **Metal removal, %** | | | | **97** | **98** |

A disadvantage of the hot vapour filtration was the reduction in organic liquid yield by approximately 5-10 wt% and increased the gas yield. Higher filtration temperature reduced more the organic liquid yield and therefore 360 °C appears to be the most suitable filtration temperature. Also, higher filtration face velocity and lower vapour phase residence time in the filter seems to increase the organic liquid yield.

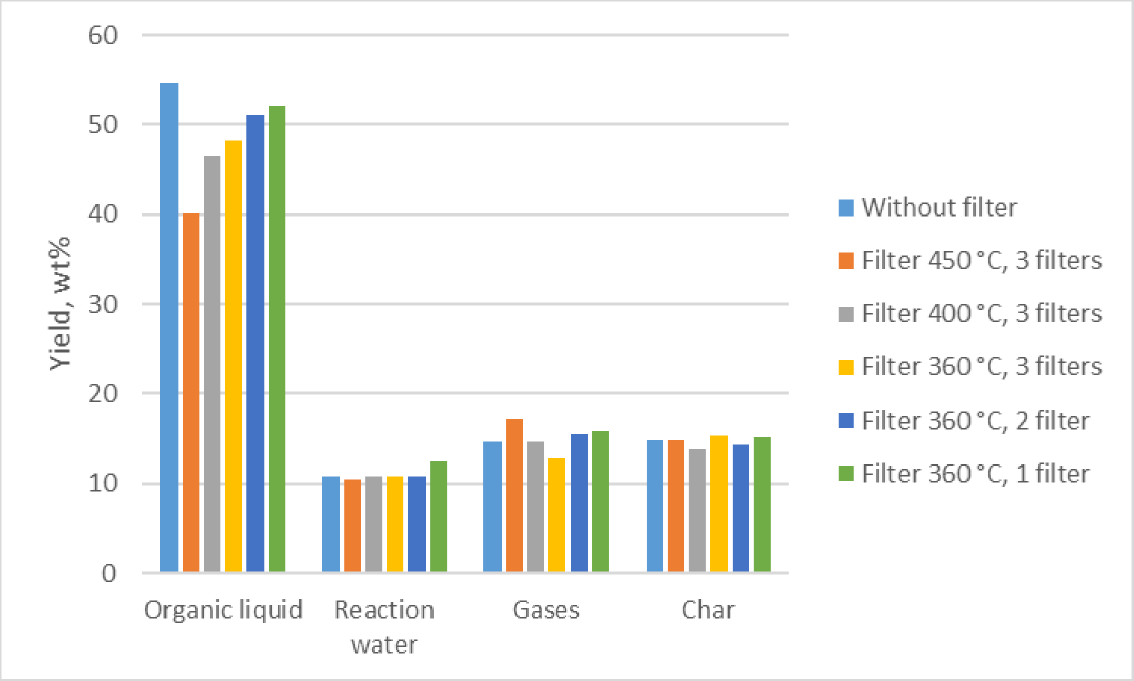

*Figure 3.2. Pyrolytic products yields at different filtration temperatures, filter face velocities and filter residence times.*

## 3.3 Pyrolysis and impurity removal of industrial residual (contaminated) wood at BTG

At BTG experiments were performed to remove inorganic contaminants from pyrolysis oil. The main objective is to understand if and how organic contaminants as organic sulfur, and inorganic materials (inorganic sulfur and ash) affect catalyst in subsequent stabilisation and deoxygenation processes and reduce catalyst deactivation. Typical compounds of interest and relevant adsorbents include ion-exchange using Ni or Cu based materials for the sulfur, and Amberlyst ion-exchange resins for any alkalis.

In these tests, packed bed reactors, operable in various designs allowing ambient or high pressures and a range of temperatures (20 to 400 ºC) are filled with the dedicated adsorbent. Pyrolysis liquids are pumped through the reactor (if relevant under hydrogen atmosphere).

For sulphur removal, other promising adsorbentia have been identified based on adsorbents from copper/nickel mixtures. Breakthrough curves are recorded. Typical removal efficiencies are in the range of 50-60 %, while absolute sulfur removal on the absrobentia is typically < 0.5 wt.%. Further tests are ongoing. Typically, Amberlyst-like resins - in cation and anion form were used to remove (alkali) metals. The objective was to remove, respectively, the positively and negatively charged ions from the pyrolysis oil. Initial results show that the content of K, Ca, Cl and S can indeed be decreased by ion exchange.

Dedicated – quick and dirty- analysis was done using an XRF unit from PANalytical using dedicated Omnian software. The results indicated that the specific software is not always fully applicable for some of the lower contaminant concentrations in pyrolysis liquids, nevertheless, the accuracy in the trends of the XRF measurements for these components appeared satisfactory for the present applications.

Typical plots for sulfur removal are summarised below, for both sulfur removal using a nickel based adsorbent at high pressures and temperatures, and alkali removal over resins at ambient conditions. In all these plots the concentrations from the XRF are taken as is, but it should be clearly stated here that those values are not the actual or 'real' values but relative, while 'calibration' of the XRF has not been succesful yet.

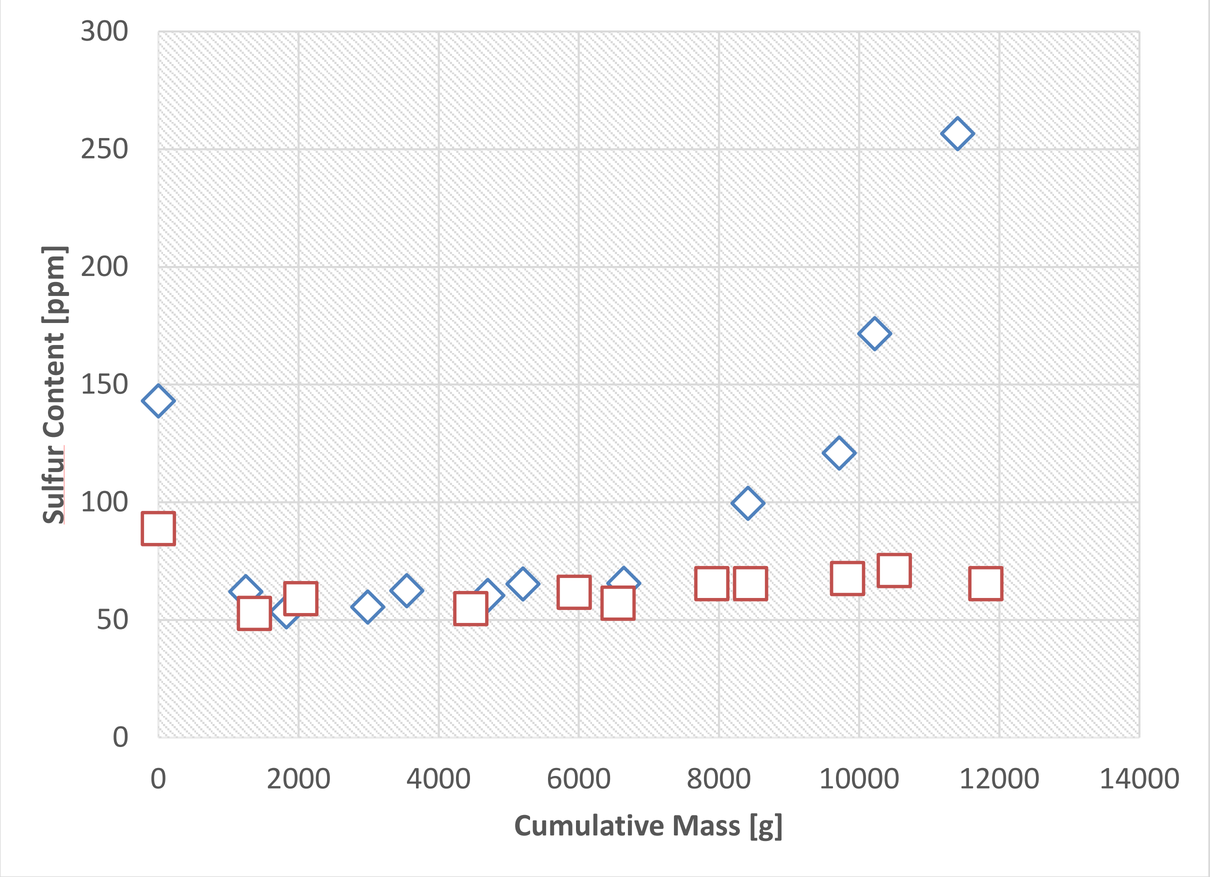

*Figure 3.3. Desulfurisation of clean wood (□) and contaminated wood oil (◊) versus the oil fed at 200 bar $H_2$ and max 120$^o$C.*

The desulfurisation performance is around 50% for clean wood (going from relatively values of 100 ppm down to 50 ppm), while for the contaminated wood is around 70% (150 ppm down to 50 ppm). In both cases sulfur remains in the pyrolysis oils, and this may suggest that part of the sulfur is there in different structures and forms. Likely, the presence of salts of sulphates that are not adsorbed on those adsorbents may be the root cause. Clearly, and as expected, the breakthrough of sulfur depends on the initial concentration. The capacity of the adsorbent (based on the relatively sulfur levels) is around 1 g sulfur per 100 g adsorbent.

For the resin testing BTG started with screening cat ion exchange experiments on water /salt mixtures, and subsequently experiments were performed on pure oils from contaminated. A 1000 ppm $Ca(OH)_2$ solution was successfully tested to confirm that Ca were removed from the feed (<50 ppm). In a subsequent experiment, the commercial cation resin was tested using the pyrolysis liquid (Figure 3.4). The concentration of Ca in the pure oil (around 200 ppm) was reduced to < 30 ppm but slowly increased in time. The bed was 'saturated' at around 1100 min (50 bed volumes) with respect to Ca, where the mass of biooil collected at the end of bed life was roughly 2.5 L. Further experiments, also with a commercial anion exchange and combinations of cation and anion are required, also to investigate slightly elevated temperatures (50°C). Not shown here is the concentration of sulphur, but this was measured to see if sulphur leaches from the resin into the oil, but this could be excluded.

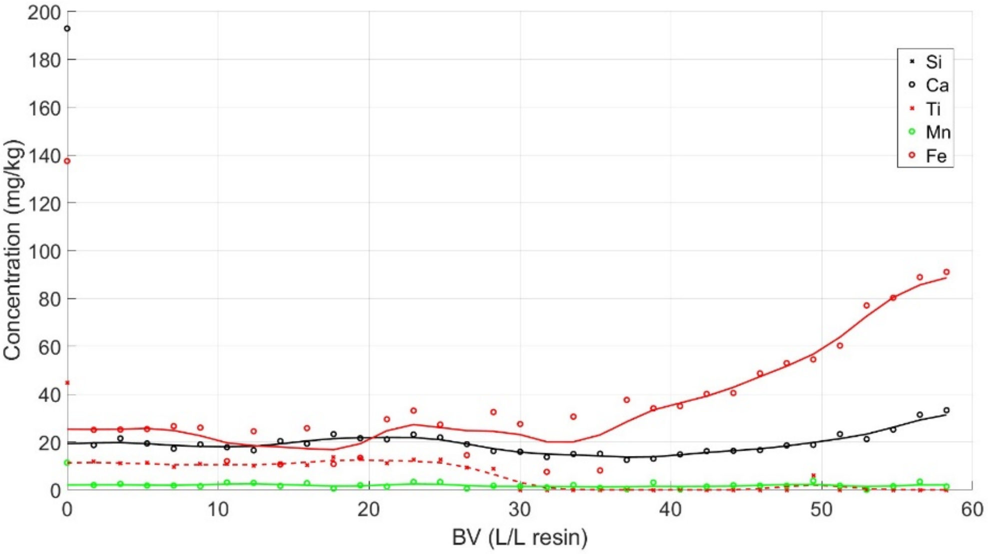

*Figure 3.4: Concentration of metals in the outlet of a resin bed, as a function of bed volumes (l oil per L of resins).*

A slow climb in iron and calcium concentrations in Figure 3.4 nearing breakthrough suggests that the kinetics of bulk to particle and/or intraparticle diffusion of ions are a limiting factor in resin efficiency. Whilst this run had obtained a higher overall removal efficiency than with an earlier up flow tests the 'sharpness' of concentration breakthrough was much less pronounced. The breakthrough is spread out over 20+ BV instead of 2 to 3 BV in earlier tests. Interestingly, iron seems to have a much lower affinity towards the resin than calcium, suggested by the larger slope in concentration.

Also, anionic experiments were done, but less numerous than for the cations, and anionic resins indeed are effective in removing some measurable anionic contaminants from contaminated FPBO in a single pass (Figure 3.5). A typical max. loading close to 40% of the theoretical maximum is expected. Additionally, P was identified as another potential anionic contaminant as it showed a decrease consistent with other ionic contaminants. P will be assumed to be present as $PO_4^{3-}$ in calculations. S and Cl are assumed to be $SO_4^{2-}$ and $Cl^-$, respectively.

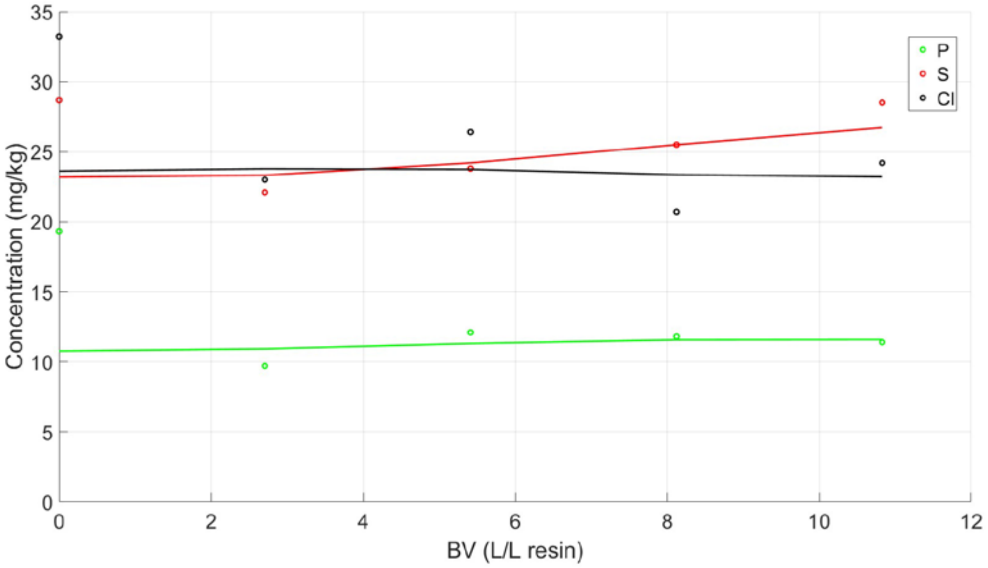

*Figure 3.5: Anionic contaminants concentration in the contaminated wood oil as a function of bed volumes (l oil per L of anion resins).*

Some cation resin regeneration experiments were done (not yet on the anion). Fouling of the resin was observed, that could not be cleaned afterwards (even not with acetone, or other more aggressive materials).

Finally, and on basis of the test carried out a larger of nearly 10 kg was made of a material from contaminated that was first cation exchanged, and then led over the an-ion resin. Analysis is ongoing, similarly as tests over BTG's" Picula" catalyst to stabilise the product. Results will be compared with fresh, untreated contaminated wood oils, and with this information more targeted research into catalyst longevity may be possible.

## 3.4 The effect of contaminants on fast pyrolysis process

CNRS studied the effect of contaminants on fast pyrolysis by preparing model contaminated biomasses (Figure 3.6).

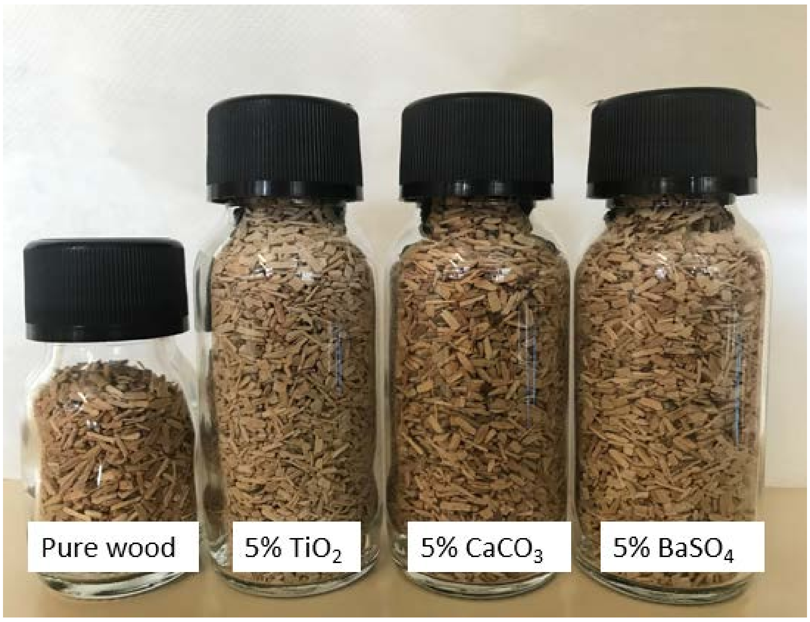

*Figure 3.6. Sample preparation: 1h of stirring in rotavapor apparatus (room temperature and atmospheric pressure), Removal of water at 50 °C and 400 mbar, Dry at room temperature at fume hood for 3 days, Water/biomass ration: 750mL/200g (3.75 mL/g), Total contaminated biomass produced: 200g*

Contaminated wood from VTT and BTG were analysed for metals by SEM-EDS and XRF at CNRS (Tables 3.7-3.9). When compared to clean wood it was obvious that Ca, K, Mg, S, and Mn were originated from wood and Ti, Si, Fe, Al, and Na were impurities in contaminated wood, Si most probably from dirt/earth. By XRD it was suggested that the inorganic compounds in contaminated wood were CaCO3, TiO2, CaO, and BaSO4, which are similar to those found in varnish and paints.

*Table 3.7. Characterization of ashes by SEM-EDS and XRF at CNRS*

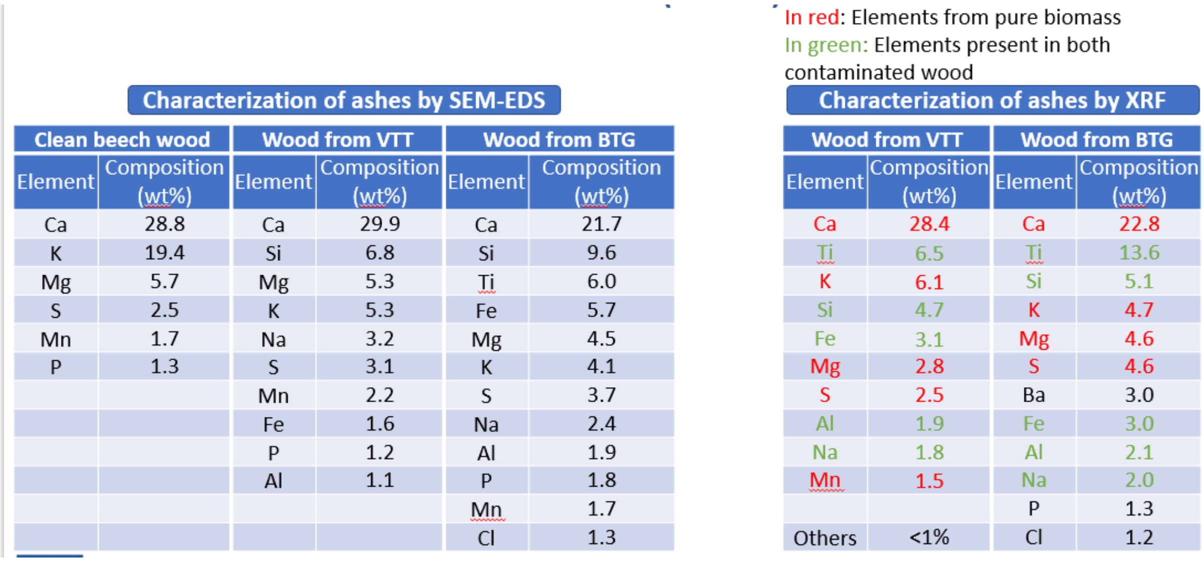

In red: Elements from pure biomass
In green: Elements present in both contaminated wood

**Characterization of ashes by SEM-EDS**

| Clean beech wood | | Wood from VTT | | Wood from BTG | |
|---|---|---|---|---|---|
| Element | Composition (wt%) | Element | Composition (wt%) | Element | Composition (wt%) |
| Ca | 28.8 | Ca | 29.9 | Ca | 21.7 |
| K | 19.4 | Si | 6.8 | Si | 9.6 |
| Mg | 5.7 | Mg | 5.3 | Ti | 6.0 |
| S | 2.5 | K | 5.3 | Fe | 5.7 |
| Mn | 1.7 | Na | 3.2 | Mg | 4.5 |
| P | 1.3 | S | 3.1 | K | 4.1 |
| | | Mn | 2.2 | S | 3.7 |
| | | Fe | 1.6 | Na | 2.4 |
| | | P | 1.2 | Al | 1.9 |
| | | Al | 1.1 | P | 1.8 |
| | | | | Mn | 1.7 |
| | | | | Cl | 1.3 |

**Characterization of ashes by XRF**

| Wood from VTT | | Wood from BTG | |
|---|---|---|---|
| Element | Composition (wt%) | Element | Composition (wt%) |
| Ca | 28.4 | Ca | 22.8 |
| Ti | 6.5 | Ti | 13.6 |
| K | 6.1 | Si | 5.1 |
| Si | 4.7 | K | 4.7 |
| Fe | 3.1 | Mg | 4.6 |
| Mg | 2.8 | S | 4.6 |
| S | 2.5 | Ba | 3.0 |
| Al | 1.9 | Fe | 3.0 |
| Na | 1.8 | Al | 2.1 |
| Mn | 1.5 | Na | 2.0 |
| | | P | 1.3 |
| Others | <1% | Cl | 1.2 |

*Table 3.8 Characterization of ashes by XRF and XRD at CNRS*

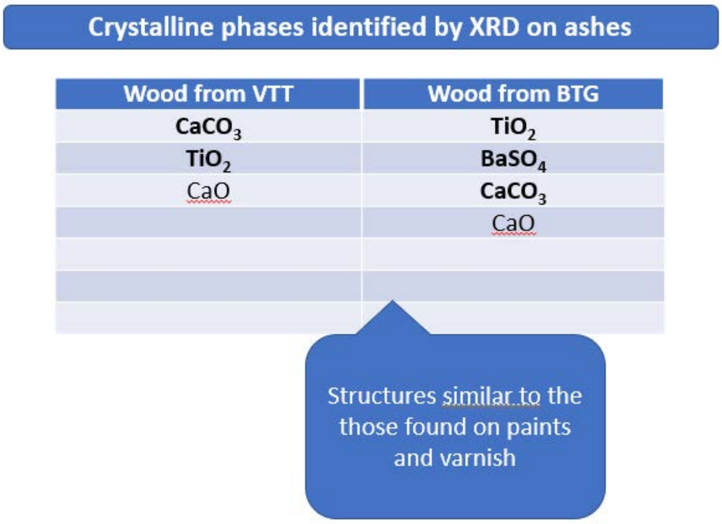

**Crystalline phases identified by XRD on ashes**

| Wood from VTT | Wood from BTG |
|---|---|
| **$CaCO_3$** | **$TiO_2$** |
| **$TiO_2$** | **$BaSO_4$** |
| CaO | **$CaCO_3$** |
|  | CaO |
|  |  |
|  |  |
|  |  |

Structures similar to the those found on paints and varnish

*Table 3.9. Contaminant's characterization (CNRS)*

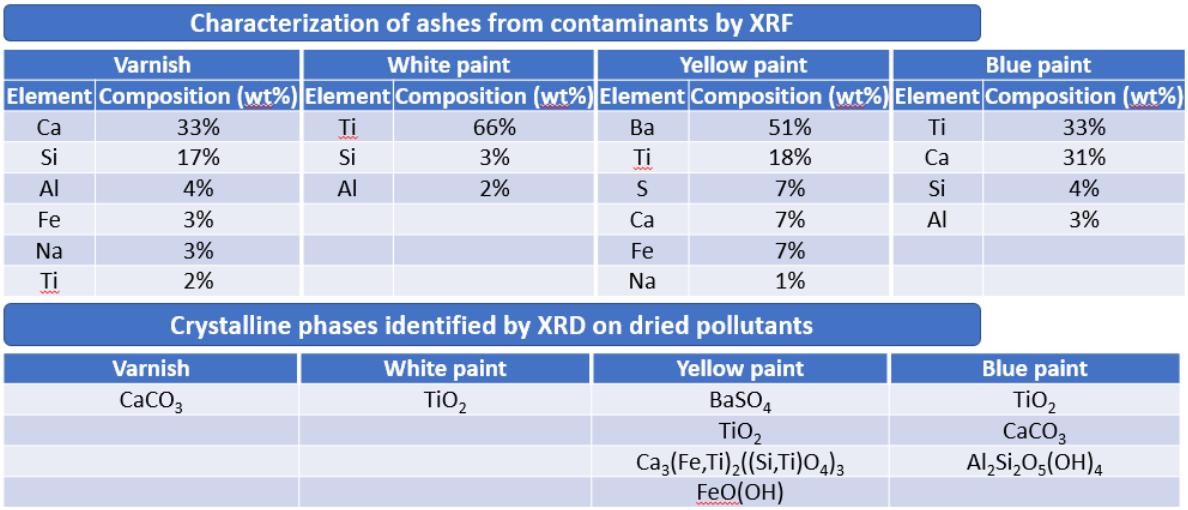

**Characterization of ashes from contaminants by XRF**

| Varnish |  | White paint |  | Yellow paint |  | Blue paint |  |
|---|---|---|---|---|---|---|---|
| **Element** | **Composition (wt%)** | **Element** | **Composition (wt%)** | **Element** | **Composition (wt%)** | **Element** | **Composition (wt%)** |
| Ca | 33% | Ti | 66% | Ba | 51% | Ti | 33% |
| Si | 17% | Si | 3% | Ti | 18% | Ca | 31% |
| Al | 4% | Al | 2% | S | 7% | Si | 4% |
| Fe | 3% |  |  | Ca | 7% | Al | 3% |
| Na | 3% |  |  | Fe | 7% |  |  |
| Ti | 2% |  |  | Na | 1% |  |  |

**Crystalline phases identified by XRD on dried pollutants**

| Varnish | White paint | Yellow paint | Blue paint |
|---|---|---|---|
| $CaCO_3$ | $TiO_2$ | $BaSO_4$ | $TiO_2$ |
|  |  | $TiO_2$ | $CaCO_3$ |
|  |  | $Ca_3(Fe,Ti)_2((Si,Ti)O_4)_3$ | $Al_2Si_2O_5(OH)_4$ |
|  |  | FeO(OH) |  |

Results of XRF confirmed the presence of elements (such as Ti, Fe, Ba, Si…) in contaminated wood. Identification of main structures present on ashes using XRD, confirming that oxides used to impregnate the biomass (TiO2, CaCO3 and BaSO4) are representative of contaminated wood. The presence of pollutants resulted in:

- Phase separation of liquid phase obtained for reaction without catalyst (as similarly obtained with catalyst)
- Reduction in average molar mass
- Increase in aromatic and unsaturated compounds
- Reduction in sugars, acids and esters.

The contaminants modified the reactivity of wood particles.

## 3.5 HTL of Food wastes and impurity removal at CEA

Hydrothermal Liquefaction experiments were carried out on the food wastes collected at the company restaurant H1 at CEA Grenoble. Biocrudes are the raw product produced by hydrothermal liquefaction. The biocrude can be separated into char and bio-oil via solvent extraction. The results of these analyses have been presented in D3.7. In the tables below (Tables 3.10 and 3.11), we focus on elements that can be considered as a pollutant.

*Table 3.10. Properties of biocrude values (and there standard deviations).*

| **Feedstock description** | **Unit** | **Sulphur Content** | **Nitrogen Content** | **Ash Content** |
|---|---|---|---|---|
| Food Waste | Batch Reactor | 0.22 (0.09) % | 3.4 (0.7) % | 3.8 (1) % |
| FFOM | Batch Reactor | 1.8 % | 0.9 % | 40 % |
| Soda Black Liquor | Batch Reactor | 0.07 (0.03) % | 0.2 (0.2) % | 34 (15) |
| Kraft Black Liquor | Batch Reactor | 1.2 (0.1) % | 0.1 (0) % | 0.1 % |
| Food Waste | Continuous Reactor | 0.21 (0.05) % | 2.4 (0.6) % | 1.4 % |

As biocrude is a mixture of char and bio-oil, it concentrates water insoluble ashes. Certain resources are rich in ash such as FFOM and black liquor. Much of this ash ends up with the char in the biocrude. The extracted bio-oil was also analysed for ashes. A small amount of ash was detected visually but the quantity was too small to be quantified by weighing. The ash fraction of the bio-oil is less than 0.1%.

*Table 3.11. Properties of biocrude values (and their standard deviations).*

| **Feedstock description** | **Unit** | **Na** | **K** | **Mg** | **Ca** |
|---|---|---|---|---|---|
| Food Waste | Batch Reactor | 0.12 (0.2) % | 0.1 (0.1) % | 0.08 (0.03) % | 1.2 (0.5) % |
| FFOM | Batch Reactor | 0.3 | 0.3 | 0.8 | 5.5 |
| Soda Black Liquor | Batch Reactor | 15 % | 0.1 % | 0.1 % | 1.5 % |

The ash in the biocrudes contains small amounts of alkalis such as sodium and potassium. Salts with a limited solubility in water tend to dominate in biocrude ashes such as magnesium and calcium.

## 3.6 Validation of sampling and analyses

To follow the pathway of contaminants it is important to have proper sampling and accurate analytical methods. More detail information is included in D3.7 A summary report of properties of bio-liquids.

### 3.6.1 Homogenisation and sampling

A protocol for homogenisation and sampling is suggested for validation:

- All samples will be homogenised/mixed properly
- Samples will be halfed immediately after mixing by rapid pouring
- Samples will be mixed for 30 minutes
- These two samples will be again halfed immediatedly after mixing by rapid pouring
- All four samples will be mixed for 30 min and samples for water, CHN, Cl, S, solid and ash (VTT rapid method MCR+ash) analyses taken

- If adequate accuracy/repeatability of the results all samples are sent to ICP analyses as different samples. Importance of proper mixing and rapid sampling will be informed to the laboratory. Also, possible level of alkali/earth alkali and other metals will be discussed with the laboratory to enable proper calibration. Data on calibration will be requested.
- If NOT adequate accuracy/repeatability of the results the homogenization and sampling procedure will be modified

### 3.6.2 Analyses

FPBO was analysed for water, C, H, N, Cl, S, solids, MCR and ash according to – ASTM methods using bio-oil from: Sunflower oil, Grass pellet oil organic phase, Grass pellet oil aqueous phase, and bio-oil from contaminated wood. The relative standard deviations (12 duplicates) for water, MCR, carbon, hydrogen and chlorine were < 5 % and for solids, ash, nitrogen and sulphur < 11 %.

*Table 3.12. Analyses for FPBOs*

| | Water, ASTM E203 | | | Solids, ASTM D7579 | | | MCR, ASTM D4530 | | | Ash, Combustion of MCR | | |
|---|---|---|---|---|---|---|---|---|---|---|---|---|
| Sample | Average, wt% | SD, wt% | RSD, % | Average, wt% | SD, wt% | RSD, % | Average, wt% | SD, wt% | RSD, % | Average, wt% | SD, wt% | RSD, % |
| Sunflower oil | 32.0 | 0.3 | 1.1 | 0.5 | 0.1 | 10.6 | 15.4 | 0.1 | 0.9 | 0.2 | 0.0 | 7.1 |
| Grasspellet organic phase | 14.8 | 0.5 | 3.6 | 1.5 | 0.0 | 1.9 | 14.3 | 0.5 | 3.7 | 0.6 | 0.1 | 8.3 |
| Grasspellet aqueous phase | 72.6 | 0.3 | 0.4 | | | | 2.9 | 0.1 | 2.8 | 0.3 | 0.0 | 6.2 |
| Contaminated wood | 19.3 | 0.2 | 1.0 | 0.2 | 0.0 | 4.8 | 24.2 | 0.4 | 1.6 | 0.1 | 0.0 | 3.9 |

*Table 3.13. Elemental analyses for FPBOs*

| | Carbon, ASTM D5291 | | | Hydrogen, ASTM D5291 | | | Nitrogen, ASTM D5291 | | | Sulfur, ASTM D5453 | | | Chlorine, modified ASTM D4929 | | |
|---|---|---|---|---|---|---|---|---|---|---|---|---|---|---|---|
| Sample | Average, wt% | SD, wt% | RSD, % | Average, wt% | SD, wt% | RSD, % | Average , wt% | SD, wt% | RSD, % | Average, mg/kg | SD, mg/kg | RSD, % | Average, mg/kg | SD, mg/kg | RSD, % |
| Sunflower oil | 39.8 | 0.6 | 1.5 | 8.1 | 0.1 | 0.8 | 0.9 | 0.0 | 4.7 | 1224.8 | 70.3 | 5.7 | 149.9 | 6.9 | 4.6 |
| Grasspellet organic phase | 61.2 | 0.3 | 0.6 | 9.4 | 0.1 | 0.7 | 5.2 | 0.1 | 1.6 | 6352.9 | 308.0 | 4.8 | 318.7 | 10.9 | 3.4 |
| Grasspellet aqueous phase | 13.9 | 0.1 | 0.5 | 10.0 | 0.1 | 0.7 | 3.3 | 0.1 | 1.5 | | | | | | |
| Contaminated wood | 44.4 | 0.1 | 0.2 | 7.2 | 0.1 | 1.2 | 0.5 | 0.0 | 9.0 | 323.7 | 7.2 | 2.2 | 394.5 | 3.4 | 0.9 |

## 3.7 HCN formation during fast pyrolysis of biomass and wastes

New waste derived feedstocks have awakened interest to investigate the safety of the operation of fast pyrolysis units and the analysis protocols. Nitrogen present in fast pyrolysis feedstock can contribute to the evolution of highly toxic and harmful components, which can end up in the product or into working environment in case if equipment malfunction or during maintenance. Especially HCN evolution during the pyrolysis has been under concern due to its high toxicity and harmfulness to humans and environment already in low concentrations.

HCN evolution from fuels have been studied largely from combustion point-of view where $NO_x$ emissions are concern. $NO_x$ can be formed by thermal oxidation of $N_2$ to $NO_x$, evolution from Fuel-N (HCN as intermediate and oxidized to $NO_x$), or prompt N from the $N_2$ (HCN as intermediate and oxidized to NOx). Relevant pathways from the point-of view of pyrolysis is the HCN evolution from Fuel-N and the prompt N. In pyrolysis the HCN is not oxidized due to the lack of oxygen in the system.

Nitrogen containing substance of biomass are mostly proteins, but also free amino acids, alkaloids, nucleic acids, nitrates, amines, inorganic-N, and chlorophyll-N. Specific components are highly dependent from the type of biomass. Adhesives and resins in wood products are nitrogen sources in contaminant/demolition wood. Nitrogen content of heartwood is typically low (< 0.2 wt%). Needles and bark contain more nitrogen (< 0.6 wt%). Some biobased waste fractions (such as coffee waste and wastewater sludges high in proteins) can contain up to 8 wt% nitrogen.

N distribution was determined in a fast pyrolysis experiment with sawdust. Over 50wt% of N was bound in FPBO, 30-40% was in gas phase (possibly as HCN and NH3) and less than 10 wt% in char. (VTT internal results)

Becidan et al. (9) studied N pathway in pyrolysis by model compounds (Table 3.14) and HCN formation during fast pyrolysis of fibreboard, coffee waste and brewery waste (Figure 3.7). They found out that main gaseous nitrogen products are NH3 and HCN (and N2), conversion to NH3 and HCN increases with increasing temperature (highest conversion 46 – 52 % was reached in 825 - 900 ˚C), and with fibreboard very small concentrations of HCN below 700 ˚C can be detected.

*Table 3.14. Model compounds versus biomass: Literature results from pyrolysis.*

|  | model compounds |  |  |
|---|---|---|---|
|  | amino acids and proteins | pyrrole- and pyridine-type | biomass |
| N-components | HCN, $NH_3$ and HNCO for all model compounds and biomass |  |  |
| fuel intrinsic properties influence | functional groups favors the formation of $NH_3$ |  | no clear correlation |
| fuel physical properties influence | higher heating rates appear to increase HCN/$NH_3$ ratio |  |  |
| mechanistic comments | main intermediates are cyclic amides (most common: 2,5-diketopiperazines) formed by dehydration | main intermediates are nitriles formed by ring opening | see model compounds; however, results are difficult to interpret because of the complex N-compounds makeup in biomass and their possible interactions with other biomass compounds (cellulose, hemicellulose, lignin) |
| main N-component | HCN major compound for most compounds, else $NH_3$ | HCN major product and almost only product at high temperatures (> 1000 ˚C) | sometimes HCN, sometimes $NH_3$ |
| char production | compounds with side-chains or extra functional side groups produce char |  | significant amount of char produced |
| $NH_3$-HCN release: operating parameters | increasing N-release with increasing temperature and heating rates |  | increasing release with increasing temperature and heating rate for HCN but conflicting results for $NH_3$ |
| $NH_3$ release | correlation between char and $NH_3$ production |  | char formation appears to be important for $NH_3$ formation |

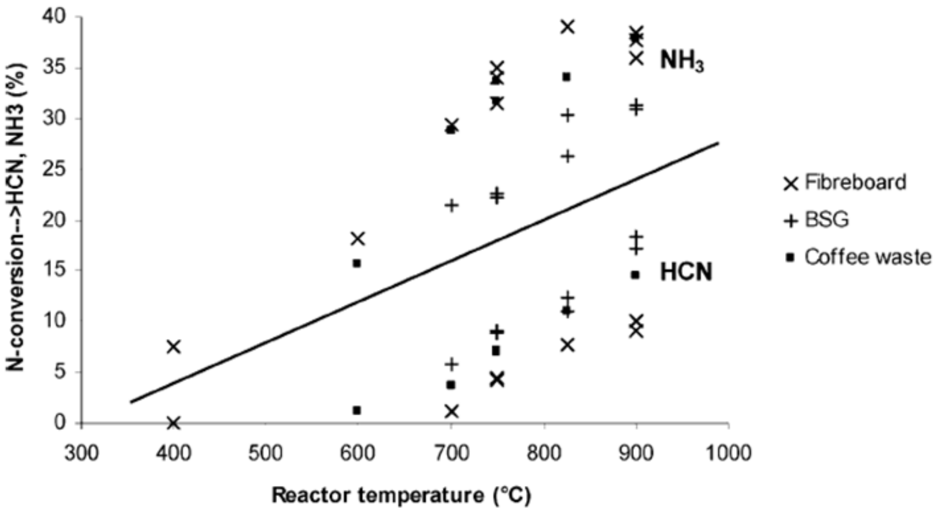

*Figure 3.7. N-conversion to HCN and NH3: high heating rate experiments.*

Fuel analyses and risk assessment must be done before any experiments. High nitrogen content in feedstock is a risk. Analytical pyrolysis is a good tool to assess the product spectrum when needed, especially when there is new type of feedstocks with high uncertainty, or high nitrogen content feedstocks.

It can be concluded that HCN formation is highly dependent on the feedstock type and nitrogen content, but also process conditions. Generally, HCN formation is favoured by high temperatures and high heating rates. (9) Fast pyrolysis and fluidized bed units are characterized with high heating rates, but all experimental reactors are not. No HCN has been observed from fibreboard pyrolysis under 600 ˚C. On the other hand, significant amount of HCN from sludges has been measured already at 500 ˚C.

# 4 Conclusions and recommendations

The objective of the task 3.6 was to investigate the effect of different contaminants present in biomass (such as in the contaminated wood or in municipal wastes) on the quantity and quality of the primary bio-oils and downstream fuels.

Contaminated wood from VTT and BTG were analysed for metals by SEM-EDS and XRF at CNRS. When compared to clean wood it was obvious that Ca, K, Mg, S, and Mn were originated from wood and Ti, Si, Fe, Al, and Na were impurities in contaminated wood, Si most probably from dirt/earth. By XRD it was suggested that the inorganic compounds in contaminated wood were CaCO3, TiO2, CaO, and BaSO4, which are similar to those found in varnish and paints.

By model compound (biomass added with contaminants) study at CNRS it was concluded that the presence of pollutants resulted in:

- Phase separation of liquid phase obtained for reaction without catalyst (as similarly obtained with catalyst)
- Reduction in average molar mass
- Increase in aromatic and unsaturated compounds
- Reduction in sugars, acids, and esters.

The contaminants modified the reactivity of wood particles. Hence, it is obvious that the impurities must be removed already during primary processes.

Besides metals, chlorine, and sulphur contents are often high in the primary oils from waste materials. Most of the metals are removed in the pyrolysis process together with the char in the cyclones. Hot vapour filtration can be added to the process to remove rest of the pollutants. This is important for the downstream upgrading, like HDO, where the catalyst can deactivate due to impurities, like potassium. In the new filter concept developed by VTT fast pyrolysis vapors did not block the pores of the filter due to the moving bed / barrier filter. Because of the increase in vapour residence time and activity of alkali and other metals hot vapor filtration reduces the organic liquid yield by approximately 10 % and increases the gas yield. Lower filter temperature and higher face velocity minimized the decrease in organic liquid yields. The hot-vapour filtration did not significantly affect the oil properties.

Also ex-situ techniques using Ni or Cu based materials for the sulfur, and Amberlyst ion-exchange resins for any alkalis removal were studied in packed bed reactors in the project. The desulfurisation performance is around 50% for clean wood (going from relatively values of 100 ppm down to 50 ppm), while for the contaminated wood is around 70% (150 ppm down to 50 ppm). In both cases sulfur remains in the pyrolysis oils, and this may suggest that part of the sulfur is there in different structures and forms.

For the resin testing BTG started with screening cat ion exchange experiments on water /salt mixtures, and subsequently experiments were performed on pure oils from contaminated wood. The concentration of Ca in the pure oil (around 200 ppm) was reduced to < 30 ppm but slowly increased in time. The bed was 'saturated' at around 1100 min (50 bed volumes) with respect to Ca, where the mass of biooil collected at the end of bed life was roughly 2.5 L. Further experiments, also with a commercial anion exchange and combinations of cation and anion are required, also to investigate slightly elevated temperatures ($50^oC$).

Biocrudes produced by hydrothermal liquefaction are a mixture of bio-oil and char. Water insoluble salts such as $SiO_2$, $FeCO_3$, $CaCO_3$, etc, tend to be associated to the char, increasing its volume. Solvent extraction will help to reduce the inorganics from the bio-oil to very small concentrations. Distillation may be more effective, but this has not been tested.

Inorganics in biocrude produced from black liquor consist mainly of sodium that can be washed with water.

# 5 References

1. A Guide to Physical Property Characterisation of Biomass-Derived Fast Pyrolysis Liquids.. Oasmaa, A.; Peacocke, C. VTT Publications: Espoo, Finland, 2010; VTT Publications, Vol. 731, ISBN: 978-951-38-7384-4, http://www.vtt.fi/inf/pdf/publications/2010/P731.pdf.
2. Norms, Standards, and Legislation for Fast Pyrolysis Bio-Oils from Lignocellulosic Biomass. Oasmaa, A.; van de Beld, B.; Saari, P.; Elliott, D. C.; Solantausta, Y. Energy & Fuels 2015, 29 (4), 2471–2484. https://doi.org/10.1021/acs.energyfuels.5b00026
3. A Guide to Physical Property Characterisation of Biomass-Derived Fast Pyrolysis Liquids.. Oasmaa, A.; Peacocke, C. VTT Publications: Espoo, Finland, 2010; VTT Publications, Vol. 731, ISBN: 978-951-38-7384-4, http://www.vtt.fi/inf/pdf/publications/2010/P731.pdf.
4. Physical characterisation of biomass-based pyrolysis liquids: Application of standard fuel oil analyses. Oasmaa, A.; Leppämäki, E.; Koponen, P.; Levander, J.; Tapola, E.; VTT Publications 306; VTT: Espoo, Finland, 1997; 46 pp + app. 30 pp. (ISBN 951-38-5051-X). http://www.vtt.fi/inf/pdf/publications/1997/P306.pdf.
5. Results of the IEA Bioenergy Round Robin on the Analysis of Heteroatoms in Biomass Liquefaction Oils. Philip Bulsink, Ferran de Miguel Mercader, Linda Sandström, Bert van de Beld, Fernando Preto, Alan Zacher, Anja Oasmaa, Magnus Marklund, Nicolaus Dahmen, Axel Funke, Benjamin Bronson. Energy Fuels 2020, Publication Date:August 6, 2020, https://doi.org/10.1021/acs.energyfuels.0c02090
6. Results of the IEA Round Robin on Viscosity and Stability of Fast Pyrolysis Bio-Oils. Elliott, D. C.; Oasmaa, A.; Preto, F.; Meier, D.; Bridgwater, A. V.. Energy & Fuels 2012, 26 (6), 3769–3776. https://doi.org/10.1021/ef300384t.
7. Results of the IEA Round Robin on Viscosity and Stability of Fast Pyrolysis Bio-Oils. Elliott, D. C.; Oasmaa, A.; Preto, F.; Meier, D.; Bridgwater, A. V. Energy & Fuels 2012, 26 (6), 3769–3776. https://doi.org/10.1021/ef300384t
8. Norms and Standards for Fast Pyrolysis Liquids 1. Round Robin Test. Oasmaa, A.; Meier, D. J. Anal. Appl. Pyrolysis 2005, 73 (2), 323–334. https://doi.org/10.1016/j.jaap.2005.03.003
9. Becidan, M., Skreiberg, Ø., & Hustad, J. E. (2007). Energy and Fuels, 21(2), 1173–1180

**Appendix 1 – XRF**

A substantial amount of work has been performed by BTG in analysing in X-ray fluorescence (XRF) is a measurement technique wherein an outside source of electromagnetic radiation is used to bombard a sample. If an electron is successfully knocked out from one of the inner orbitals of an atom of the target material then another electron from one of the outer orbitals will take its place. In doing so this second electron will emit a photon with an energy equal to the energy difference between these two orbital layers. Since every type of element has unique energy differences between their various orbitals every single element can theoretically be qualitatively identified by the unique fluorescence pattern of their photon emissions. Depending on the concentration of these elements in the sample the quantity of these photons that are detected will change thus giving a quantitative analysis as well.

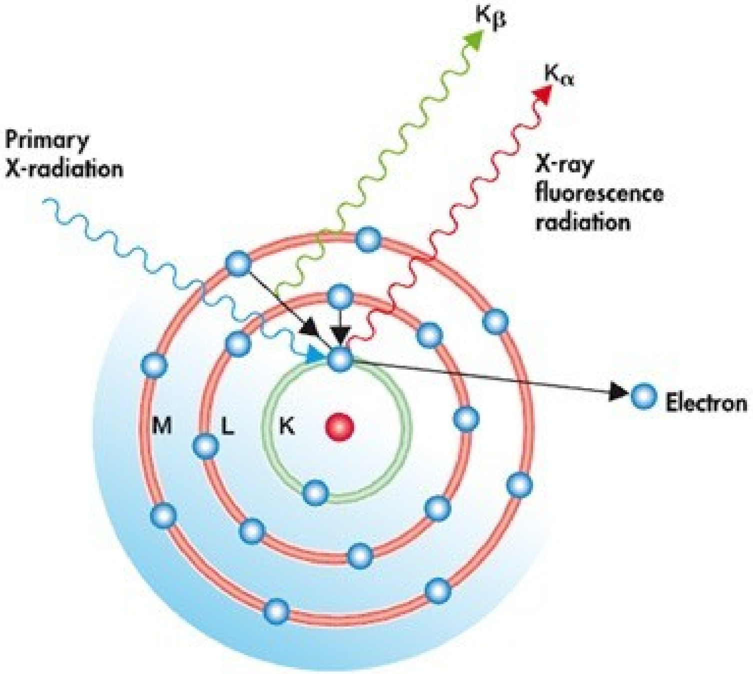

Figure 1. X-ray fluorescence.

Besides the fluorescence there are two more modes of emission possible. Compton scattering occurs when an electron in the outer orbitals is ’hit’ by the incoming photon. The product is an ejected electron and a photon that has lost a small part of its energy to this interaction. This type of scattering usually occurs with lighter elements as the electrons in the outer shells are typically less strongly bound to the atom. Rayleigh scattering occurs when a photon comes into contact with a tightly bound electron, if the electron remains in orbit it will eventually release the absorbed energy as a photon identical to the incoming radiation. Giving the appearance of reflecting the incoming radiation. Besides these modes of emission there are certain other effects that may occur that have consequences on the results. As photons enter the detector some signals may enter within such a short time span that they are seen as a single peak.

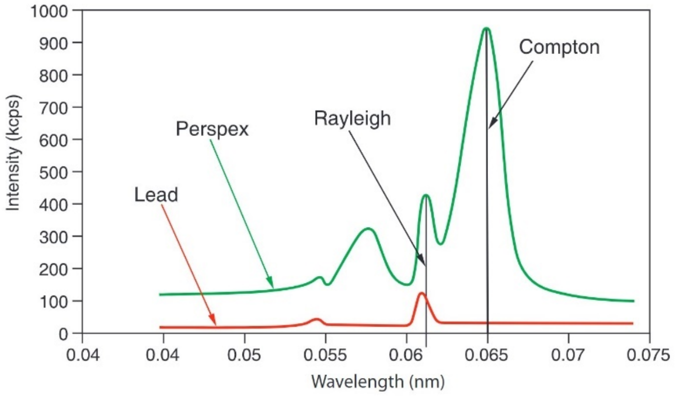

Figure 2: Example of Rayleigh and Compton scattering.

These artefacts are called sum peaks and produce a false signal equal to the sum energy of the two separate photons. Escape peaks occur when atoms from the detector itself are ionised by the incoming photons, if the resultant photon is detected then it will have an energy equal to the original incoming radiation minus the energy used up to ionise the atom in the detector.

With the current tuning of the XRF setup at BTG the following spectra were obtained using a standard-less simulation based analysis of the sample spectra.

Table 1: Typical raw XRF data of water and unprocessed FPBOs in mg/kg

| | Demineralised water | Contaminated wood FPBO | Finland batch FPBO |
|---|---|---|---|
| Mg | | | |
| Si | ~~696~~ | 761 | 445 |
| P | 12 | 30 | 9 |
| S | | 216 | 31 |
| Cl | 66 | 495 | 62 |
| Ca | 1 | 164 | 14 |
| Ti | | 22 | |
| Mn | | 12 | 2 |
| Fe | 8 | 118 | 9 |
| Co | | | |
| Ni | 22 | 56 | 53 |
| Cu | 98 | 152 | 147 |
| Zn | ~~642~~ | 853 | 959 |
| Zr | 2 | 2 | 3 |
| Mo | 1 | 3 | 2 |
| Pd | ~~57~~ | | |
| Cd | ~~34~~ | 44 | 43 |
| Sn | ~~32~~ | 13 | 28 |
| Eu | | 4 | |
| Dy | ~~48~~ | | 94 |
| Er | ~~76~~ | | |

| | |
|---|---|
| Re | 1 |
| Pb | 1 |

From this table it should be clear that the values obtained through XRF are not necessarily the true concentrations in the measured samples. It is highly unlikely that demineralised water contains over 600 ppm of both silica and zinc as well as traces of rare earth metals such as palladium. As such the quantities obtained cannot be taken as absolute and must be considered in relation to other measurements. For continuity sake the method used will not be changed during the experiments, this should allow for easier comparison of results between the various experiments. In calculating things such as resin loading and efficiency the numbers obtained through XRF will be used as absolute.